OPTICAL DEPOLARIZATION CHANGES ON THE DIFFRACTION PATTERN IN THE TRANSITION OF SKINNED MUSCLE FIBERS FROM RELAXED TO RIGOR STATE

Y. YEH, M. E. CORCORAN, R. J. BASKIN, AND R. L. LIEBER
Department of Applied Science and Zoology Department, University of California, Davis, California 95616

ABSTRACT Light diffraction spectra from single or small bundles of skinned striated muscle fibers show large changes in polarization properties when muscles are placed into rigor. The technique of combining optical diffraction and ellipsometry measurements has previously been shown by Yeh and Pinsky to be a sensitive probe of periodic anisotropic regions of the fiber. In the present work, using this method, the observed spectrum shows marked decrease in the measured phase angle, δ, as the fiber approaches the rigor state. The degree of phase angle change is a function of sarcomere length: Maximum overlap of ~2.3 μm gives the most change in δ a $\Delta\delta_{R\text{-}R} \sim 35°$ decrease for a bundle of three fibers. At a sarcomere length of 2.9 μm this $\Delta\delta_{R\text{-}R}$ value is only 10°. At a nonoverlapping length of ~3.8 μm, δ does not vary at all upon the removal of ATP. The rigor state was confirmed by stiffness measurements made after small-amplitude (0.75%), quick length changes. Upon re-relaxation, the stiffness of the skinned fiber decreased to the value of the resting state (4 mM ATP) and the phase angle δ returned to its original value. A model based on either anisotropic subunit-2 (S-2) movements or other cross-bridge–related structural anisotropy (form birefringence) changes during the relaxed-rigor transition is suggested.

INTRODUCTION

Muscle contraction at the sarcomere level involves the conversion of chemical energy into mechanical energy. The mechanical movement leads to actual shortening of the sarcomere length. The sliding filament theory (1, 2) for sarcomere shortening states that the thick myosin filaments slide past the relatively thin f-actin filaments. The point where mechanical force generation affects the sliding motion is generally thought to be at the site where the actomyosin complex is formed (3). Because electron microscopic (4) and small-angle x-ray diffraction (5) data support the existence of a myosin moiety (S-1) that shifts its location from the thick filament during the resting state to the actin filament upon contraction, cross-bridge movement by the heavy meromyosin (HMM) parts of the thick filament toward the thin filament have been postulated. Motion of the S-1 element has been the subject of investigation in several experiments using fluorescent (6) and phosphorescent (7) tags, electron spin labels (8), as well as x-ray scattering using a synchrotron source (9).

It is difficult to monitor and assess the importance of the possible dynamics of the S-2 moiety of the myosin rod whose behavior in solution shows rather large angular orientation capabilities (10). In the present experiment, the technique of optical ellipsometry (11) has been used to measure changes in the optical polarization signal of the diffraction patterns from single skeletal fibers or bundles of three fibers. In a previous publication (12), we reported on the ellipsometry measurements of diffraction patterns upon passive stretch of an intact fiber. This technique provides more spatial selectivity of anisotropic elements in that only those elements with sarcomere periodicity will exhibit the diffraction pattern. In this work, these studies have been extended to measure changes in optical polarization of the diffraction pattern when a fiber goes from the relaxed state to the rigor state, where all the available cross-bridges are attached. We have been able to correlate the changes in the ellipsometry measurement with changes in both the diffraction intensity and the mechanical stiffness of the fiber to consistently put a single fiber into rigor and then release the rigor condition upon reintroducing chilled 4 mM ATP to the solution. In almost all cases reported here, the ellipsometry measurements are reversible, as are diffraction intensity and stiffness. From these results, we shall discuss the source of the changes in the depolarization signal when the fiber undergoes the relaxed-rigor transition.

Dr. Lieber's current address is the Division of Orthopedics, Veterans Administration Hospital, University of California, San Diego, CA 92161.

EXPERIMENT

Background of Technique

When a light wave traverses a medium that is optically anisotropic, the plane of polarization will change. The amount of change and the type of change depend upon the material traversed. Generally, a linearly polarized light beam will develop elliptical polarization; the extent and nature of this elliptically polarized light is determined by the polarizabilities along the various material axes and the relative phase relationship between these axes at this optical wavelength. When this measurement is performed on the diffraction pattern from a muscle fiber, optically anistropic elements with the spatial regularity of the sarcomere are measured. Fig. 1 provides a schematic diagram of the apparatus used in this experiment. Linearly polarized laser light at 0.633 μm was sent through the stage containing the fiber. The polarization direction of incident light was controlled by a half-wave plate. Diffracted light from the fiber was collected at either first or second order through a collection system consisting of a rotating quarter-wave plate and a final polarizer followed by a photomultiplier. The detected intensity was recorded as a function of the angle of the fast axis of the quarter-wave plate. Because the dominant anisotropic element within the sarcomere is within the A-band, and because the myosin S-2 element is by far the most anisotropic of all the sarcomeric elements that could change orientation upon activation, we discuss the changes in ellipsometry measurements based on the dynamics of S-2 elements below. The S-2 element, like the LMM, is composed of an α-helix (13). Because the α-helix has ~3.6 residues per pitch, upon excitation electron movement transverse to the helical axis was significantly faster than along the helical axis. Accordingly, light traversing the diameter of such an anisotropic region (Fig. 2 *a*) experiences a relative optical pathlength difference. A linearly polarized light beam becomes elliptically polarized; the degree of ellipticity is dependent upon polarizabilities $\alpha\|$ and $\alpha_\perp$, and upon δ, the phase shift between these axes. If one imagines that the rod is now tilted so that the axis of the rod is along the propagation direction of the light beam, linearly polarized light no longer experiences optical anisotropy and will remain linearly polarized (Fig. 2 *b*). In general, we would expect a decrease in δ upon simple tilt of this anisotropic rod (Fig. 2 *c*). Because the rod is assumed not to denature, the magnitude of the polarizabilities remains fixed, thus both $\alpha\|$ and $\alpha_\perp$ must remain constant.

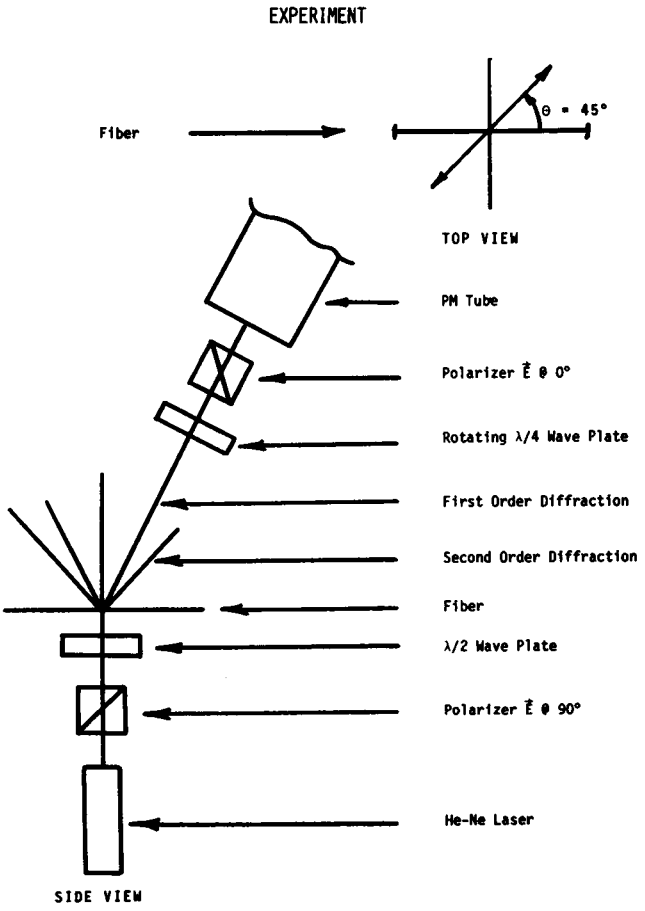

FIGURE 1 Schematic representative of the actual optical apparatus for measuring the polarization properties of diffracted light.

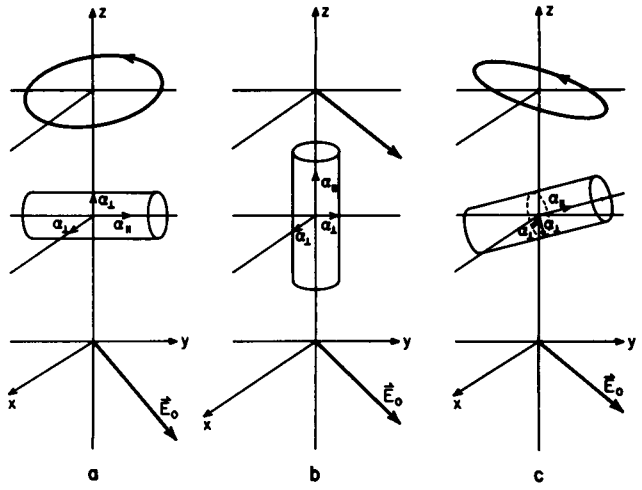

FIGURE 2 Schematic representations of how the anisotropic element ($\alpha_\|$, $\alpha_\perp$, $\alpha_\perp$) converts incident linearly polarized light (along z-axis) to elliptically polarized light. (*a*) Element lying in the horizontal plane, (*b*) element standing straight up, (*c*) element at a tilt angle with respect to the horizontal.

In this experiment, δ, $\alpha\|$, and $\alpha_\perp$ were measured by an apparatus outlined above and previously described in detail by Yeh and Pinsky (12). Using that system, elliptically polarized light appeared as a signal, such as that shown in Fig. 3, and the three fiber parameters, $\alpha\|$, $\alpha_\perp$, and δ were measured as described in reference 12.

Experimental Procedure

The lateral head of the anterior tibialis muscle from *Rana pipiens* was used in all these experiments. Skinned, single fibers are placed on a micromanipulator-controlled, cooled (~4°C) stage where light was incident through the bottom (Fig. 1). The samples were first bathed in 4 mM ATP relaxing solution. The sarcomere length (SL) of the fiber was then fixed by measurement of the position of the first-order diffraction maximum. The general quality of the fiber was checked with a stereo microscope with a 40× objective. The illuminated section was chosen for its uniformity in fiber diameter, absence of foreign particle adherents, and absence of visible damage. For sheets of these fibers, the tilt angle of the plane of the sheet was also checked. Several washes of the fiber at each ATP concentration were used to assure complete changes in ATP concentration and repeatability of the effect of washes. Measurements of the diffraction intensity and phase shift were then taken at successively lower ATP concentrations: 4, 2, 1, 0.5, 0.25, and 0 mM. At this last stage, the fiber was in rigor. A maximum of 20 min was allowed in this state before 4 mM ATP solution was reintroduced. The control measurement of ellipticity at the last condition constituted the completion of a single experiment.

Solution Compositions

Ringer's solution was made up of 115 mM NaCl, 2.5 mM KCl, 2.15 mM Na_2HPO_4, 0.85 mM NaH_2PO_4, and 1.8 mM $CaCl_2$; adjusted to pH 7.0. Relaxing solution was as in Julian (14): 100 mM KCl, 1 mM $MgCl_2$, 2 mM EGTA in 10 mM imidazole buffer at pH 7.0. 4 mM ATP was added just before use. Skinning solution was made by altering the Magid and Reedy skinning solution (15) for whole fibers to skin the sarcolemma of single fibers without otherwise damaging the system. This solution contained 0.125% (by volume) Triton X-100 in the above-described relaxing solution.

Skinning Procedure

A single fiber or fiber bundle was first dissected in Ringer's solution. The undamaged fiber or bundle of fibers was next soaked for at least 30 min in relaxing solution with 4 mM ATP. This procedure rids the membrane area of excess Na^+ ions, which, if present, will cause the fiber(s) to depolarize when placed in skinning solution.

After this procedure, the fiber or bundle was submerged in skinning solution containing 4 mM ATP for exactly 5 min. The duration of exposure was chosen so that only surface membrane would be disrupted. Using 10 mM caffeine activation, the sarcoplasmic reticulum was shown to be intact (16). The removal of the fiber from the skinning solution required care that no excess skinning solution remained. The fiber was first placed in relaxing solution with ATP. Repeated rinsing with fresh relaxation solution with ATP for a few minutes was necessary to rid the fiber of residual Triton X-100.

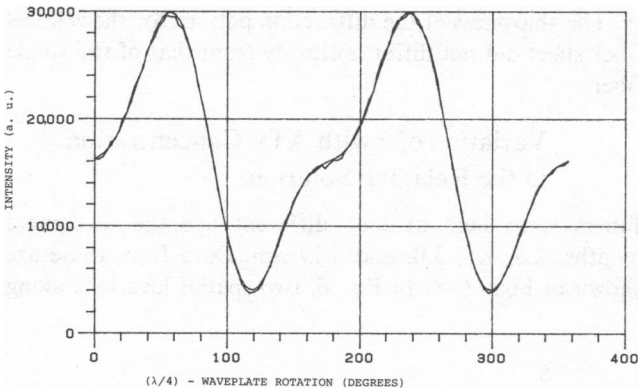

FIGURE 3 Typical intensity, I in arbitrary units (a.u.), vs. ¼-wave plate rotation.

TABLE I
PARAMETERS GOVERNING FIG. 3

A	*DA*	*S*	*DS*	*P*	*DP*
33,366.62	44.29	34,443.31	93.24	130.23	0.22
−1,775.79	62.64	−2,153.38	164.09	179.69	1.05
−8,747.36	62.64	−17,721.22	125.94	195.92	0.96
831.14	62.64	−20,950.30	62.74	Ratio = 0.80	

$\theta = 17.56°$ Initial wave-plate angle = $1.14° \pm 0.09°$ $\chi^2 = 1.71$ $r = 0.04$

θ is the diffraction angle. Initial wave-plate angle is that of the ¼-wave plate. A and DA are fit parameters and variances to the data; S and DS are the Stoke's parameters and variances. (See reference 12, Eq. 11.) P and DP are the phase angles δ, $\alpha_\parallel$, and $\alpha_\perp$, and their variances, respectively. (See reference 12, Eq. 12, a, b, c.) χ^2 is the goodness of fit parameter, and r is the polarization ratio as defined by Eq. 1. Rotation was over 360°.

Solution Change Procedure

Aluminum foil clips were used to support the tendon region on either end of the fiber (17). The clips were mounted onto pins of the micromanipulator. The chamber that contained the fiber was bathed with relaxing solution that contained the desired concentration of ATP. Each time a solution change was desired, the chamber was flushed four or five times with the appropriate solution, and experiments commenced only after a waiting period of 10 min. Repeatability of the optical experiments was assured by conducting experiments using solution rinses of the same ATP concentration. The entire chamber was maintained at ~4°C by flowing coolant that was thermostatically controlled by a constant-temperature bath.

Stiffness Measurement Procedure

The system used for the measurement of mechanical stiffness was fully described by Lieber and Baskin (18). Briefly, the single fiber was placed between a high-speed motor (step changes complete <500 μs) and tension transducer (sensitivity, 0.51 mV/mg; resonant frequency, 3.54 kHz). Experimental control and data acquisition were provided by the digital system described by Lieber et al. (19). Diffraction data were obtained (yielding sarcomere length values) every 270 μs. After the fiber had been bathed in the desired ATP solution for at least 10 min, a rapid step change in length was applied to one end of the fiber. Stiffness was expressed as the force change per unit imposed length change (in neutrons per meter). The magnitude of the length change was always <0.75%, to prevent the cross-bridges from being torn off. At least two rapid stretches were imposed for each value of ATP concentration.

The mechanical response of the fiber was recorded on a storage oscilloscope, photocopied, and analyzed. The diffraction data were stored on a floppy disk for later analysis via an interactive FORTRAN program. After analysis the data were plotted using a digital plotter.

RESULTS

Variation of Phase Angle with Sarcomere Length in Passive Stretch of Skinned Single Fiber or a Bundle of Three Fibers

Fig. 4 displays the phase angle (δ) variation with sarcomere length of relaxed fiber. Two experiments, one on a skinned single fiber and the other on a sheet of three fibers, were recorded. When the latter's δ-value was normalized to the δ-value of the single fiber of diameter ~70 μm at SL of 2.3 μm, both decreasing slopes were very similar to the control experiment using an intact fiber (also shown in the figure).

Because these skinned fibers still contained much of the SR membrane structure, the results of Fig. 4 indicate that the reason for the decrease in the value of δ upon sarcomere length change in both the intact and the skinned fiber must be similar. In Yeh and Pinsky (12) we concluded that simply decreasing the thickness of the sarcomere upon stretch is insufficient to explain this result because $\alpha\|$ and $\alpha_\perp$ did not change upon stretch. Consequently this effect may be due either to rearrangement of intrinsically anisotropic elements or to alteration of pure form birefringence by other stacked elements exhibiting sarcomere periodicity.

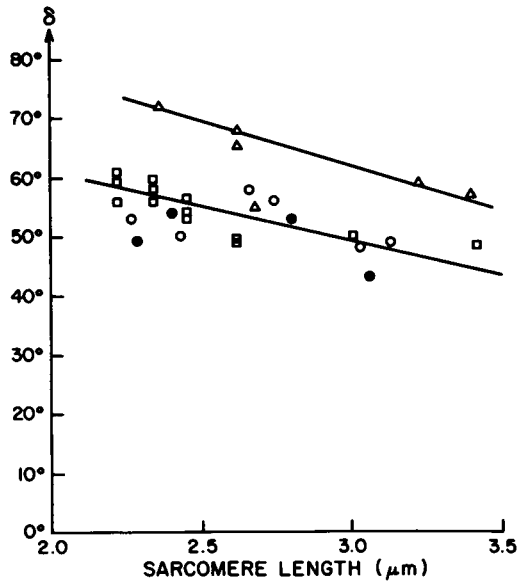

FIGURE 4 Phase angle plotted against sarcomere length. (△) represents data from an intact fiber. (□) represents data from a skinned single fiber. (○) and (●) represent data from a skinned triple fiber in the vertical and horizontal orientation, respectively. The vertical orientation data was normalized by the technique shown in Fig. 5.

Variation of δ with the Tilt Angle of the Sheet of Three Fibers

To enhance the optical path length difference, and therefore δ, we conducted most of the experiments using three fibers lying in a vertical plane as a parallel sheet of fibers. When the sheet lay horizontal in the tray, the effective optical pathlength was that of a single fiber. When the sheet stood vertically in the tray, so that light traversed successively through all three fibers, the measured phase angle corresponded to the sum of the three fibers. Fig. 5 exhibits the variation of δ with tilt angle from the horizontal position for different regions along the fiber sheet. It was seen that as the tilt angle increased, more of the sheet was traversed by the light beam, and the δ-value correspondingly increased. The monotonic increase of δ upon tilting suggested that phase-angle rotation had not gone beyond 360°. An estimate of an absolute intrinsic phase shift, $[\delta]$ ~1°/μm is obtained from these data. It is interesting to note that using the empirical relationships for optical rotation developed by Shechter and Blout (20), LMM can develop $(-6 \times 10^{-2})°$ cm³/gm − dm at λ_0 = 633 nm. All of the experiments in which ATP concentration was varied were conducted with the fiber bundle in the vertical stack. The fact that we were able to enhance optical pathlength difference in this manner implies that at least for the three-fiber case, light sequentially interacted with the fiber. Such an interaction necessarily implies multiple scattering of light and distortion of the optical diffraction pattern. To first approximation, however, the primary effect on the diffraction pattern was an alteration in the ratio of intensities of the various orders: second-order intensity increased at the expense of the first-order intensity. The sharpness of the diffraction pattern for the relaxed fiber sheet did not differ noticably from that of the single fiber.

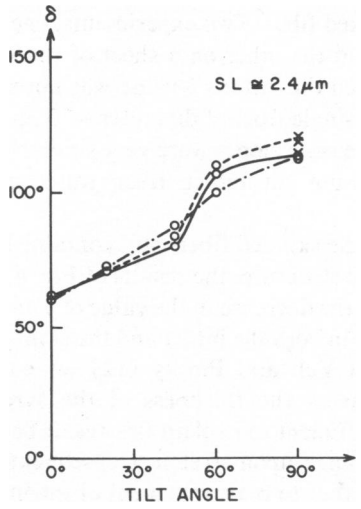

FIGURE 5 Phase angle plotted against the tilt angle of the three-fiber sheet. The tilt angle is referenced from the horizontal and represents rotation of the sheet about the long axis of the fiber. Sarcomere length is held at a constant value in this experiment.

Variation of δ with ATP Concentration in the Relaxing Solution

Fibers were held at four different average sarcomere lengths: 2.3, 2.5, 3.0, and 3.77 μm. Data from these are shown in Figs. 6–8. In Fig. 6, two spatial locations along

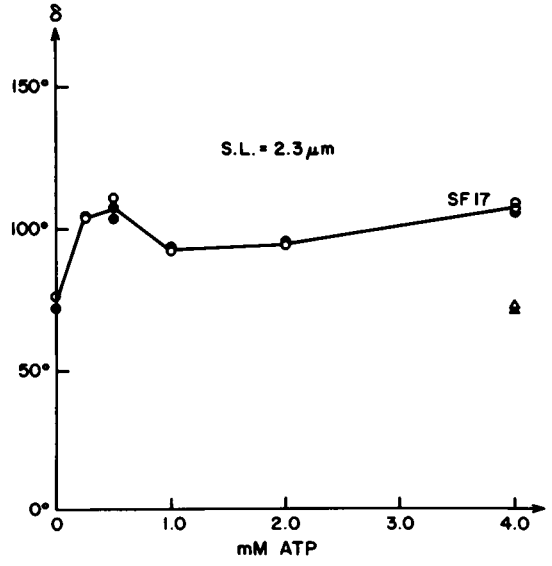

FIGURE 6 Phase angle δ plotted against [ATP] mM at sarcomere length of 2.3 μm. Two different locations on the same fiber were investigated (○) and (●). The return at 4 mM [ATP] was incomplete in this experiment (△, ▲).

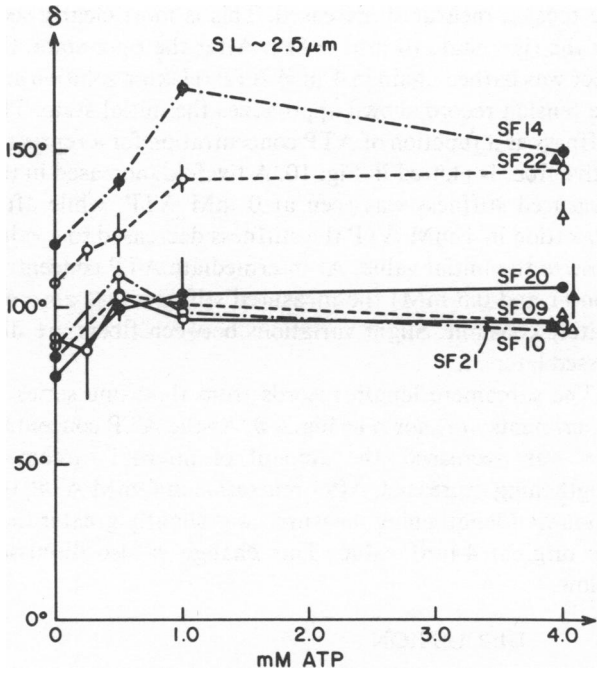

FIGURE 7 Phase angle δ plotted against [ATP] mM at sarcomere length of 2.5 μm. (○) and (●) represent data as [ATP] is reduced; (△) and (▲) represent data when 4 mM [ATP] is reintroduced.

the fiber separated by 100 μm were examined when the sarcomere length was at 2.3 μm. The consistency of these data over the distance assured us that if any rigor tension developed and the sampling region of the fiber moved by as much as 100 μm, the results were still reproducable. When ATP concentration was reduced, the most obvious trend

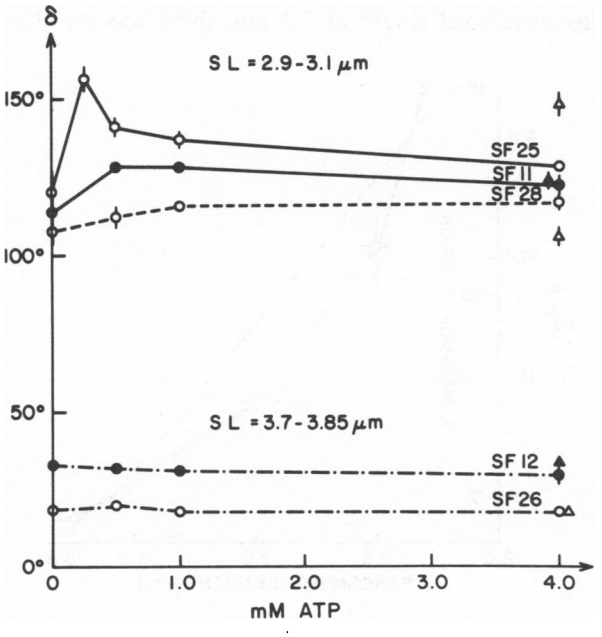

FIGURE 8 Phase angle δ plotted against mM [ATP] at 3.0 μm and ~3.8 μm sarcomere lengths. Note particularly that at the longest SL, no change in δ-value was obtained.

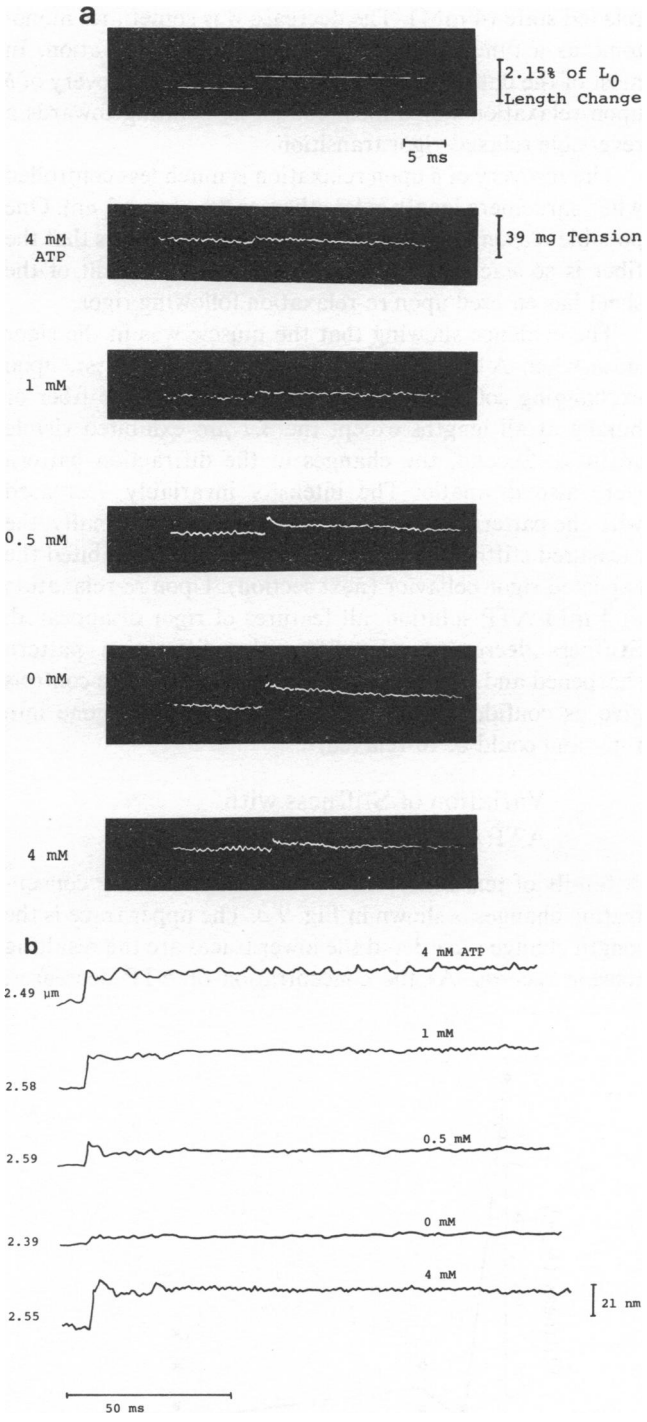

FIGURE 9 (*A*) Tension traces obtained from a single fiber given rapid stretches as ATP concentration is varied. The upper trace shows the motor movement (0.69% L_o). The remaining traces show the tension records as ATP concentration is varied (value shown at left of trace). (*B*) Sarcomere length traces associated with tension records shown in (*A*). Initial sarcomere length shown at left of trace. ATP concentration is decreased to 0 mM and then increased back to the original 4 mM concentration.

noted was that for all cases where overlap occurred, the δ-value for rigor was less than that of the value in the relaxed state (4 mM). The decrease was sometimes monotonic as a function of decreasing ATP concentration. In most of the data taken at 2.5 μm and 3.0 μm, recovery of δ upon relaxation was almost complete, pointing towards a reversible relaxed-rigor transition.

The recovery of δ upon relaxation is much less controlled when sarcomere length is less than or equal to 2.3 μm. One possible reason for this apparent lack of recovery is that the fiber is so slack at $\lesssim$2.3 μm that uncontrolled tilt of the sheet has entered upon re-relaxation following rigor.

The evidence showing that the muscle was in the rigor state when ATP was removed is as follows: First, upon exchanging solution to achieve 0 mM ATP, the fiber or bundle at all lengths except the 3.7 μm exhibited visible stiffness. Second, the changes in the diffraction pattern were also dramatic: The intensity invariably decreased with the pattern becoming much more diffuse. Finally, the measured stiffness data shown in Figs. 9–10 exhibited the expected rigor behavior (next section). Upon re-relaxation in 4 mM ATP solution, all features of rigor disappeared: Stiffness decreased, (Fig. 10), the diffraction pattern sharpened and became much more intense. These controls give us confidence that indeed our fibers had gone into rigor and could be re-relaxed.

Variation of Stiffness with ATP Concentration

A family of tension records from a series of ATP concentration changes is shown in Fig. 9 *a*. The upper trace is the length change record and the lower traces are the resulting tension records. As the concentration of ATP decreases, the tension measured increased. This is most clearly seen for the rigor state (0 mM ATP). After the rigor state, the fiber was bathed again in 4-mM ATP relaxing solution and the tension record shown approaches the initial state. The stiffness as a function of ATP concentration for a representative fiber is plotted in Fig. 10. A fivefold increased in the measured stiffness was seen at 0 mM ATP, while after relaxation in 4-mM ATP the stiffness decreased to a value close to the initial value. At intermediate ATP concentration (1 and 0.5 mM) the measured stiffness was approximately constant. Slight variations between fibers are discussed later.

The sarcomere length records from the same series of experiments are shown in Fig. 9 *b*. As the ATP concentration was decreased, the amount of internal sarcomere lengthening decreased. After relaxation in 4-mM ATP, the amount of lengthening measured was slightly greater than the original 4-mM value. This change is also discussed below.

DISCUSSION

The major result from this study is the observation that the change in phase angle upon rigor, $\Delta\delta_{R\text{-}R}$ decreased with sarcomere length of the fiber from the fully relaxed state at 2.3 μm to the nonoverlapping condition at 3.8 μm (Fig. 6–8). The values of $\Delta\delta_{R\text{-}R}$ were obtained by subtracting the δ-value at rigor from the δ-value of the fully relaxed (4 mM ATP) state, irrespective of the δ-values obtained at intermediate ATP concentrations. $\Delta\delta_{R\text{-}R}$ was then plotted against SL in Fig. 11. In attempting to interpret this result in the light of the sliding filament model, we have also exhibited the length-tension data of Gordon et al. (21) on the same figure. When normalized to the approximately fully overlapped length of 2.2 μm, there was an almost

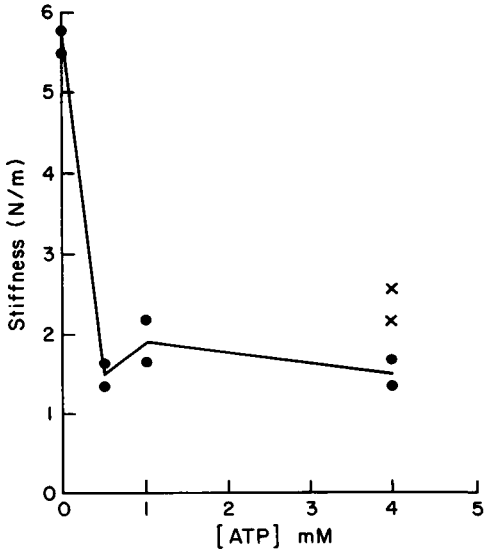

FIGURE 10 Fiber stiffness as a function of ATP concentration. Stiffness is expressed as tension per unit imposed length change. When the fiber is in the rigor state (0 mM [ATP]) the stiffness increases fivefold.

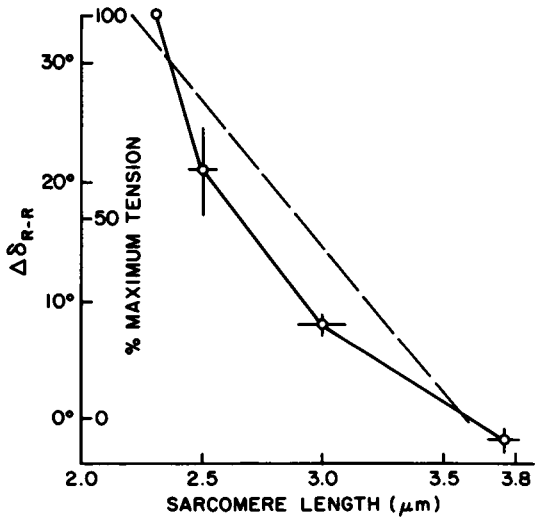

FIGURE 11 The change in phase angle, δ, between 4 mM [ATP] and rigor (0 mM [ATP]) is denoted by $\Delta\delta_{R\text{-}R}$. This is plotted against sarcomere length and compared with the percent maximum active tension data from Gordon et al. (21).

linear decrease of $\Delta\delta_{R\text{-}R}$ that paralleled the active tension produced in the descending limb of the length-tension curve. It is therefore tempting to interpret our data in terms of the number of cross-bridges available to enter the rigor state. When all cross-bridges had available sites on the f-actin filaments to bind upon rigor, we found $\Delta\delta_{R\text{-}R}$ to be largest. When the sliding filaments were pulled out more and more, the available number of cross-bridges and binding sites decreased. Correspondingly $\Delta\delta_{R\text{-}R}$ decreased to a sarcomere length of 3.8 μm. At this SL, no cross-bridge could attach to any site on the actin and thus $\Delta\delta_{R\text{-}R} \rightarrow 0$. Indeed, visually, the nonoverlapping fiber did not exhibit much rigidity upon the removal of ATP.

This study raises the question of why our phase change data so closely follow the length-tension curve. We have briefly discussed a possible origin of the depolarization signal in the Background portion of the Experiment section. The two situations represented in Fig. 2 *a* and *b* are extreme manifestations of how intrinsically anisotropic rods can change polarization of light upon its own orientational change. Even though we cannot conceive of extreme changes in orientation, it is indeed possible that the anisotropic S-2 can move from a slightly more horizontal position when relaxed to a slightly more vertical position upon rigor. There the change in the polarization will be similar in trend but smaller in values than those depicted in Fig. 2. It is important to emphasize that the decrease in $\Delta\delta_{R\text{-}R}$ here is only due to the differences between the relaxed and the rigor state since all other length variations have already been accounted for by the passive stretch results as shown in Fig. 4.

Another possible cross-bridge–related source of optical anistropy change is a change in form birefringence derived from the unique arrangement of cross-bridge heads (S-1) between the relaxed and the rigor positions. In this connection, recent spin-labelling studies (8) have led to the interpretation that S-1 moieties are randomly oriented in the relaxed state, but well ordered at a fixed tilt in rigor. This change in S-1 arrangement could lead to change in optical anisotropy. The detailed nature of possible changes in this form birefringence within the diffraction orders is currently under investigation.

The mechanical data indicate that as the ATP concentration was changed, the number of attached cross-bridges also changes. In the relaxed state, the length change (0.69% of L_0) was taken up proportionally along the length of the fiber (sarcomere length change in the relaxed state, 0.71%). The slightly higher value of sarcomere length change may be a reflection of stiffer end sarcomeres. The stiffness measured in the relaxed state was probably due mainly to the fiber itself as the tendon attachments remained relatively inextensible. At lower ATP concentrations, the tendons may themselves be extended due to the higher forces, and the stiffness measured may therefore underestimate the actual stiffness of the fiber.

The sacromere length traces provide information on the process of the relaxed-rigor transition. The increase in initial sarcomere length noted as ATP decreased from 4 to 1 mM (Fig. 9 *b*) could have been due to other cross-bridges along the length of the fiber attaching, and thereby stretching the region illuminated by the laser. As the ATP concentration decreased further, the initial sarcomere length decreased, presumably due to attachment of cross-bridges in the illuminated region. After relaxation, the amount of lengthening observed was greater than in the initial state. This was probably due to incomplete relaxation along the length of the fiber. The illuminated region might have been relaxed but was forced to extend disproportionately because some sarcomeres along the fiber length remained relatively stiff. Thus, the phase angle, which is insensitive to the condition of other saromeres along the fiber, may show a more complete recovery than the stiffness, which represents the properties of the entire length of the fiber. The known variability of the state of cross-bridge attachment along the length of fiber can be invoked to explain some of the stiffness variations in our data when the fiber was in 0.5 or 1.0 mM ATP. If the laser-illuminated local region was not in rigor, then SL could have increased at reduced concentration of ATP because of pulling in nearby regions that were in rigor, leading to an apparent increase in length and decrease in stiffness. On the other hand, if the region is locally in rigor, the measured stiffness will be high. This type of variation in stiffness exists in the data from two different fibers, presented in Figs. 9 and 10.

Even though the optical and stiffness data at intermediate ATP concentrations are somewhat variable, the effect of allowing the fiber to go fully into the rigor state (0 mM ATP) is clear. Stiffness increases in that state and these data provide independent evidence that changing the ATP concentration changes the number of attached cross-bridges and lends support to the hypothesis that the phase change observed is due to movement of structures associated with the cross-bridge.

It is important to mention that we have focused on only one entity of the three ellipticity parameters. The depolarizaton magnitudes, $\alpha_\parallel$ and $\alpha_\perp$ have also been measured in our study. However, when we examined the depolarization factor

$$r \equiv \left| \frac{\alpha_\perp - \alpha_\parallel}{\alpha_\perp + \alpha_\parallel} \right| \tag{1}$$

we found that all circumstances gave rise to only a small amount of change in r. In a simple interpretation, a constant r value implies that magnitudes of the polarizabilities along and perpendicular to the rod axis have not changed in stretch or in the transition from relaxation to rigor. Such an interpretation leads to the speculation that the rigor state itself does not cause serial elasticity changes in the S-2 region. It also suggests that the rigor-state stiffness can be achieved without phase transition within

the helical section of the thick filament. These studies indicate that ellipsometry measurements may provide a sensitive measure of the orientational changes of cross-bridge elements. Thus it may be possible to dynamically monitor cross-bridge attitude in a completely noninvasive manner, during force generation.

The interpretation that we have attempted here, though consistent with the observed data, cannot be considered an exclusive one given the paucity of experimental studies done thus far. Any alternative interpretation must account for (*a*) the periodicity of the contributing elements and (*b*) the ability of these elements to change phase value in the reported fashion without changes in the magnitudes of the polarizabilities during this transition. Most of the other intrinsically anisotropic elements, e.g., tropomyosin, are not known to exhibit enough mechanical reorientation upon the relaxation-to-rigor transition to produce the magnitude of $\Delta\delta_{R\text{-}R}$ observed. Nonperiodic but anisotropic elements such as the spatially diffuse sarcoplasmic reticulum membrane will not produce significant diffraction signals. We have further shown that nonperiodic contributions to scattering, such as those detectable between the zeroth and the first order, are isotropic (12) and do not vary either with sarcomere length variation or with the transitions from rigor to relaxed state.

The results of this study are qualitatively consistent with the interpretation afforded by Taylor (22) on birefringence studies of single fibers undergoing contraction. The primary advantage of the present technique of investigation is that by examining only the diffraction pattern, spatial selectivity further narrows down the possible contributors to these anisotropic changes.

The interpretation of our results by assigning a rectilinear, axially symmetric coordinate system for polarizabilities is obviously an approximation. Should the myofibrils be arranged in other symmetries, such as a helical arrangement in the fiber (23), the method of analysis similar to circular intensity differential scattering (CIDS) (24) may be needed to better represent this system.

Finally, closer scrutiny of the data shown in Figs. 6–8 will lead one to conjecture that during the process of chemically inducing the rigor transition in our discrete steps, many other phenomena occurred to yield higher δ values at 0.5 or 0.25 mM ATP. If our previous interpretation were to be consistent with this intermediate ATP concentration data, then at these ATP concentrations there may have been some fortuitous rearrangement of the cross-bridge elements to create a larger δ-value than either the relaxed or the rigor values. Because our measurements were averaged over long (~2 min) intervals, these arrangements must have lasted a considerable time to be repeatedly measured. A detailed study of optical anisotropy at these intermediate ATP concentrations is currently under way.

The participation by Mr. Bertram G. Pinsky during the early phase and by Mr. Z.-C. Xu during the final phase of this work is appreciated.

This work is supported in part by National Institutes of Health to Dr. Yeh under grant AM 26817.

Received for publication 9 March 1983 and in final form 11 July 1983.

REFERENCES

1. Huxley, A. F., and R. Niedergerke. 1954. Structural changes in muscle during contraction. Interference microscopy of living muscle fibers. *Nature (Lond.).* 173:971–973.
2. Huxley, H. E., and J. Hanson. 1954. Changes in the cross-striations of muscle during contraction and stretch, and their structural interpretation. *Nature (Lond.).* 173:973–976.
3. Lymn, R. W., and E. W. Taylor. 1971. Mechanism of adenosine triphosphate hydrolysis by actomyosin. *Biochemistry.* 10:4617–4624.
4. Reedy, M. F., F. C. Holmes, and R. T. Tregear. 1965. Induced changes in orientation of the cross-bridges of glycerinated insect flight muscle. *Nature (Lond.).* 207:1276–1280.
5. Podolsky, R. J., R. St. Onge, L. Yu, and R. W. Lymn. 1976. X-ray diffraction of actively shortening muscle. *Proc. Natl. Acad. Sci. USA.* 73:813–817.
6. Nihei, T., R. A. Mendelson, and J. Botts. 1974. Use of fluorescence polarization to observe changes in attitude of S-1 moieties in muscle fibers. *Biophys. J.* 14:236–242.
7. Eads, T. M., B. P. Citak, and D. D. Thomas. 1982. Phorphorescence anisotropy of eosin-labeled contractible proteins. *Biophys. J.* 37(2, Pt. 2):35a. (Abstr.)
8. Thomas, D. D., and R. Cooke. 1980. Orientation of spin-labeled myosin heads in glycerinated muscle fibers. *Biophys. J.* 32:891–906.
9. Huxley, H. E., R. M. Simmons, A. F. Faruqi, M. Kress, J. Bordas, and M. H. J. Koch. 1981. Millisecond time-resolved changes in x-ray reflections from contracting muscle during rapid mechanical transients, recorded using synchrotron radiation. *Proc. Natl. Acad. Sci. USA.* 78:2292–2301.
10. Highsmith, S., C. C. Wang, K. Zero, R. Pecora, and O. Jardetzky. 1982. Bending motions and internal motions in myosin rod. *Biochemistry.* 21:1182–1187.
11. Azzam, R. M. A., and N. M. Bashara. 1977. Ellipsometry and Polarized Light. Elsevier North-Holland, Inc., New York. 1–152.
12. Yeh, Y., and B. G. Pinsky. 1983. Optical polarization properties of the diffraction spectra from single fibers of skeletal muscle. *Biophys. J.* 42:83–90.
13. Cohen, C., and A. G. Szent-Gyorgi. 1957. Optical rotation and helical polypeptide chain configuration in α-proteins. *J. Am. Chem. Soc.* 79:248.
14. Julian, F. J. 1971. The effect of calcium on the force-velocity relation of briefly glycerinated frog muscle fibers. *J. Physiol. (Lond.)* 218:117–145.
15. Magid, A., and M. K. Reedy. 1980. X-ray diffraction observations of chemically skinned frog skeletal muscle processed by an improved method. *Biophys. J.* 30:27–40.
16. Wood, D. S. 1978. Human skeletal muscle: analysis of Ca regulation in skinned fibers using caffeine. *Exp. Neurol.* 58:218–230.
17. Ford, L. E., A. F. Huxley, and R. M. Simmons. 1977. Tension responses to sudden length change in stimulated frog muscle fibers near slack length. *J. Physiol. (Lond.)* 269:441–515.
18. Lieber, R. L., and R. J. Baskin. 1983. Intersarcomere dynamics of single muscle fibers during fixed-end tetani. *J. Gen. Physiol.* 82:347–364.
19. Lieber, R. L., K. P. Roos, B. A. Lubell, J. W. Cline, and R. J. Baskin. 1983. High speed digital data acquisition of sarcomere length from isolated skeletal and cardiac muscle cells. *Proc. IEEE.* BME-30:50–57.
20. Shechter, E., and E. R. Blout. 1964. An analysis of the optical rotatory dispersion of polypeptides and proteins. *Proc. Natl. Acad. Sci USA.* 51:695–702.

21. Gordon, A. M., A. F. Huxley, and F. J. Julian. 1966. Tension development in highly stretched muscle fibers. *J. Physiol. (Lond.)* 184:143–169, 170–192.

22. Taylor, D. L. 1976. Quantitative studies on the polarization optical properties of striated muscle. I. Birefringence changes of rabbit psoas muscle in the transition from rigor to relaxed state. *J. Cell. Biol.* 68:497–511.

23. Peachy, L. D., and B. R. Eisenberg. 1978. Helicords in the T system and striations of frog skeletal muscle fibers seen by high voltage electron microscopy. *Biophys. J.* 22:145–154.

24. Bustamante, C., M. F. Maestra, and I. Tinoco, Jr. 1980. Circular intensity differential scattering of light by helical structures. I. Theory. *J. Chem. Phys.* 73:4273–4281.